EVALUATION OF ELECTRON IMPACT EXCITATION DATA ALONG ISOELECTRONIC SEQUENCES

G. Y. LIANG,[a]* N. R. BADNELL,[b] and G. ZHAO[a]

[a]*National Astronomical Observatories, Chinese Academy of Sciences, Key Laboratory of Optical Astronomy Beijing 100012, China*
[b]*University of Strathclyde, Department of Physics, Glasgow G4 0NG, United Kingdom*

Received November 20, 2012
Accepted for Publication January 25, 2013

R-matrix calculations of electron impact excitations have been done for several isoelectronic sequences under the program of the Atomic Processes for Astrophysical Plasmas network in the United Kingdom. The intermediate-coupling framework transformation R-matrix approach was used to generate data in this program since it is less resource (time/memory) demanding than the full Breit-Pauli R-matrix method, without reduction of accuracy. A detailed accuracy assessment was done for four/five/six selected ions spanning the isoelectronic sequence, which provides insight into the behavior of the whole sequence of ions. For each ion, we adopted the following procedure: First, the target structure was assessed by comparing the calculated level energies with available experimental data and with previous calculations using different methods. Second, weighted oscillator strengths or line strengths or radiative decay rates were compared with various available theoretical works for several transitions. Usually, a "survey" comparison with another database has been done for all available transitions by way of a scatter plot. Finally, direct comparison for the excitation (effective) collision strength is done with available measurements or with previously published data. A survey comparison with another database is usually presented to investigate the spread of the consistency or inconsistency among the different calculations.

KEYWORDS: *electron impact excitation, R-matrix, data evaluation*

Note: Some figures in this paper are in color only in the electronic version.

I. INTRODUCTION

Spectroscopy provides dominant observational data in astronomy, from which we can understand the heating mechanism of hot plasmas. An example is accretion shocks from falling of circumstellar disk materials in young stars—TW Hydrae is first suggested, since it differs from a solarlike magnetic dynamo.[1] X-ray and extreme ultraviolet spectroscopy with high resolution can help us to understand the physical structure of stars by (differential) emission measure (EM/DEM). The EM/DEM distribution of the sun shows different behavior for coronal hole, quiet sun, active region, and flare.[2] Now, solar astrophysics can determine the dynamics of plasma flow and its temperature/density conditions in various regions of the sun from the high-resolution Hinode/EIS observations with the aid of spectral modeling.[3] The review paper by Güdel and Nazé presents more details about the X-ray spectroscopy of stars.[4] However, there are still large differences between the theoretical models and stellar observations in the comparison of Chianti (version 6) prediction and Procyon Chandra observation.[5] Recently, the serial works by Del Zanna and coauthors (Refs. 6, 7, and 8 and references therein) significantly improve the current Chianti model. He-like spectroscopy has been extensively used to diagnose the plasma condition, as well as to probe the heating mechanism and level populations in various celestial objects, such as in a black hole,[9] cool and young stars,[1] as well as comets.[10] However, Foster et al. revealed that there are still large differences between the new (version 2.0) and older (version 1.3.1) AtomDB models, from which the resultant temperature can be different by up to a factor of 2 even for this simple two-electron system.[11] Another example, the

*E-mail: gyliang@bao.ac.cn

line ratio of singlet ($3C$) and triplet ($3D$) 3d→2p transition lines of neonlike iron is still being debated in astrophysical and laboratory spectroscopy 30 years after its first report.[11] The discrepancy between different models can be up to ~30%. Generally, researchers attribute this discrepancy to the accuracy of fundamental atomic data, not to the model completeness.

To improve the current spectral models extensively used by the astrophysical and magnetic fusion communities [e.g., Chianti, Atomic Data and Analysis Structure (ADAS), AtomDB], the Atomic Processes for Astrophysical Plasmas (APAP) network was set up in the United Kingdom to generate accurate atomic data (including electron impact excitation) along isoelectronic sequences and to assess the reliability of the final product (via the APAP Web site, http://www.apap-network.org). In Sec. II, we present the method and atomic models in our calculations of isoelectronic sequences. The data assessment is given in Sec. III, followed by conclusions in Sec. IV.

II. CALCULATION METHOD AND ATOMIC MODELS

In our work, the intermediate-coupling framework transformation (ICFT) *R*-matrix approach was used to calculate electron impact excitation data.[12] The *R*-matrix method efficiently includes resonances usually omitted by the distorted-wave method. The ICFT variant is less resource (time/memory) demanding than the full Breit-Pauli R-matrix method, without reduction of accuracy.[13] This makes meaningful isoelectronic sequence calculations a reality within the *R*-matrix framework.[14] The target wave functions were obtained from AUTOSTRUCTURE (AS) using the Thomas-Fermi-Dirac-Amaldi model potential.[15] Relativistic effects were included perturbatively from the one-body Breit-Pauli operator (namely, mass-velocity, spin-orbit, and Darwin) without valence-electron two-body fine-structure operators. This is consistent with the operators included in the standard Breit-Pauli *R*-matrix suite of codes. Witthoeft et al. automated this complicated calculation to require less manual intervention using a Perl script[14] (see Fig. 1), which significantly benefits atomic physics researchers who use it to generate scientific atomic data for spectroscopic modeling. Liang and Badnell implement other parameters to improve its functions.[16]

So far, calculations for the He-like,[17] Li-like,[18] B-like,[19] F-like,[14] Ne-like,[16] and Na-like[20] isoelectronic sequences have been completed and the resultant data assessed. In our calculations, larger configuration interaction (CI) were included to obtain accurate target with appropriate close-coupling (CC) expansion due to computational resources, i.e., Ne-like,[16] where the 31 lowest-lying configurations were adopted in CC expansion, with an additional 33 correlation configurations—$2s^2 2p^4 3l3/4/5l'$ (l and $l' \in$ s, p, d, f, and g)—in CI expansion. For core-electron excitations, radiative and Auger damping effects were included, as in Li-like[18] and Na-like[20] isoelectronic sequences. Figure 2 shows the excitation data

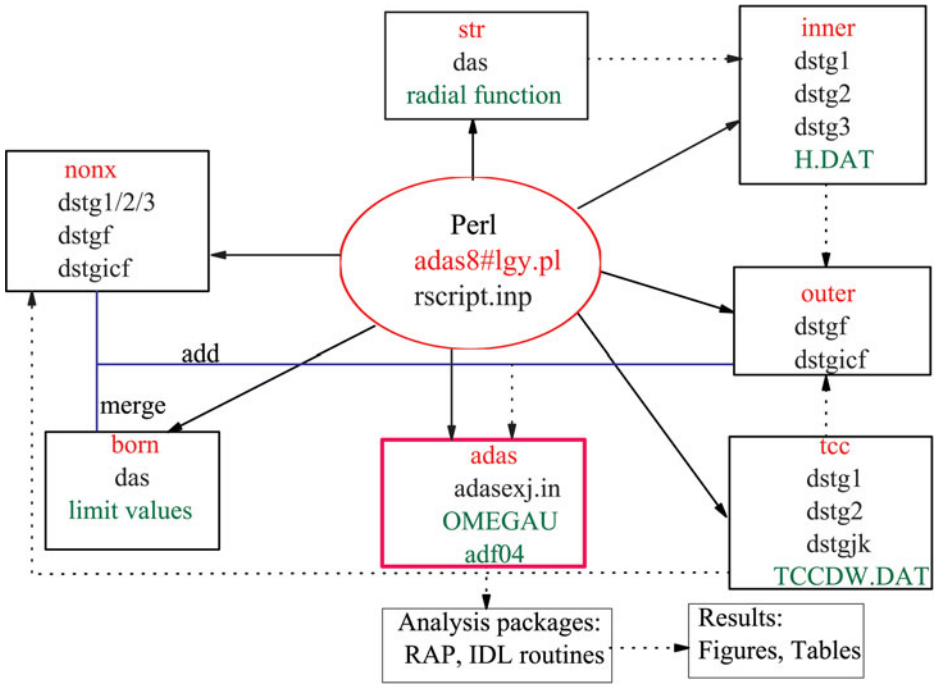

Fig. 1. Flowchart of ICFT *R*-matrix calculation. Dotted arrows denote calculation flow.

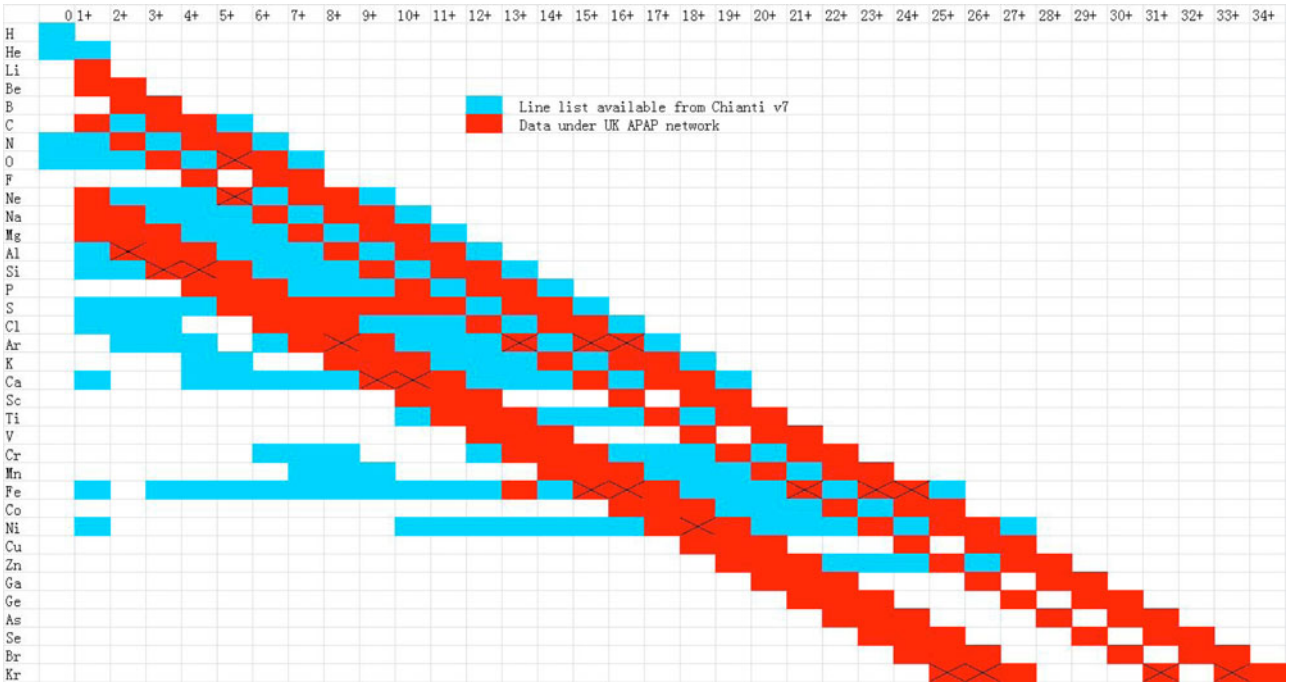

Fig. 2. Excitation data available in Chianti version 7 (Ref. 21) and in the current APAP network.

available in Chianti version 7 along with the current data in the United Kingdom's APAP network.[21] Calculations for another three isoelectronic sequences (including Be-like, C-like, and Mg-like) and some urgently important ions are planned in the second APAP program.

III. DATA ASSESSMENT

A detailed accuracy assessment was done for four/five/six selected ions (indicated by the × symbols in Fig. 2) spanning the isoelectronic sequence, which provides insight into the behavior of the whole sequence of ions. For each ion, we adopted the procedures described below.

III.A. Level Energy

First, the target structure was assessed by comparing the calculated level energies with available experimental data and with previous calculations using different methods. For Ne-like ions, the AUTOSTRUCTURE results agree well with the data from the National Institute of Science and Technology (NIST) version 3 compilation, within 0.5% (see Fig. 3). For other sequence ions, our results are also within 1% for $n = 3, 4, 5$ levels in comparison with those data from the NIST compilation and previous theories. For $n = 2$ levels, the AS results show a comparable accuracy with other theoretical calculations, within 1%, and are still within 5% in comparison

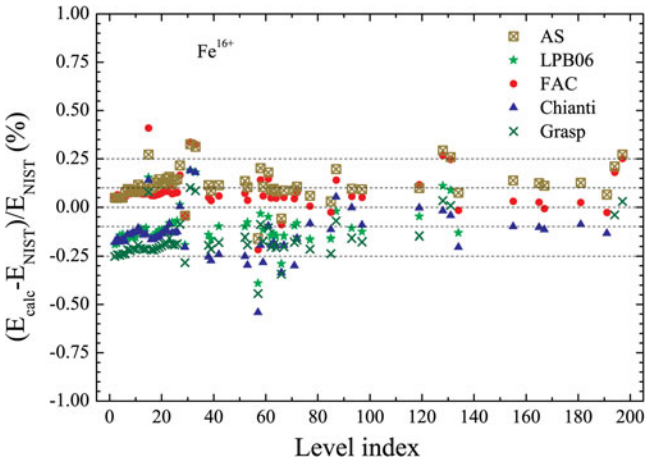

Fig. 3. Comparison of level energy of Ne-like iron ion; see Fig. 1 of Liang and Badnell's work[16] for details.

with NIST data even for the boron-like system. In this case, we perform structure calculation with level energy corrections to the diagonal of the Hamiltonian matrix to account for resonances near threshold.[19]

III.B. Oscillator Strength

Second, weighted oscillator strengths ($g_i f_{ij}$ for a given $i \leftarrow j$ transition) or line strengths (S_{ij}) or radiative decay rates (A_{ji}) were compared with various available

theoretical works for several transitions. In terms of the transition energy E_{ij} (Ryd) for the $j \rightarrow i$ transition, there are the following relations:

$$f_{ij} = \frac{E_{ji}}{3 g_i S_{ij}} \quad (1)$$

and

$$A_{ji}(\text{au}) = \frac{1}{2} \alpha^3 \frac{g_i}{g_j} E_{ji}^2 f_{ij} \ , \quad (2)$$

where α is the fine-structure constant and g_i, g_j are the statistical weight factors of the initial and final states, respectively.

Usually, a "survey" comparison with another database has been done for all available transitions by way of a scatter plot, as shown in Fig. 4 for Li-like ions. For O^{5+}, an excellent agreement is obtained between the AS results and those of the GRASP calculation: 97% of available dipole transitions agree to within 5%. For Ar^{15+}, a comparison with the previous AS (Ref. 22) and GRASP calculations has been made: ~93% and 81%, respectively, of available transitions agree to within 5%. For Fe^{23+}, 98% of available outer-shell transitions from the ADAS database show agreement to within 5% (Ref. 22). The present AS calculation also shows good agreement with the GRASP calculation—75% of available transitions show agreement to within 5%. For Kr^{33+}, somewhat worse agreement appears with previous results, which were obtained using the Dirac-Slater atomic-structure approach.[23] However, ~57% of available transitions still show agreement to within 10%. For other sequences, our results are within 20% for most dipole transitions.

Overall, the atomic structure of the ions spanning the sequence is reliable, and the uncertainty in collision strength (Ω) due to inaccuracies in the target structure is correspondingly small.

III.C. Collision Strength

Third, direct comparisons for the excitation (effective) collision strength were made with available measurements or with previously published data (see Fig. 5). For Fe^{16+}, a good agreement is obtained between our results and those of Loch et al.[24] for the background cross section (e.g., ~10% at an electron energy of 1100 eV). The cross section convoluted by a Gaussian profile (a

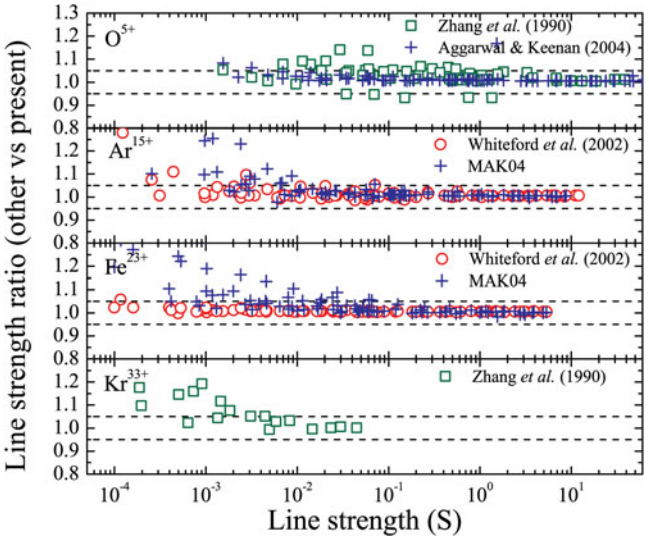

Fig. 4. Comparison of the line strength (S) of outer-shell dipole transitions for ions spanning the Li-like isoelectronic sequence. The horizontal dashed lines correspond to agreement within 5%. See Ref. 18 for details.

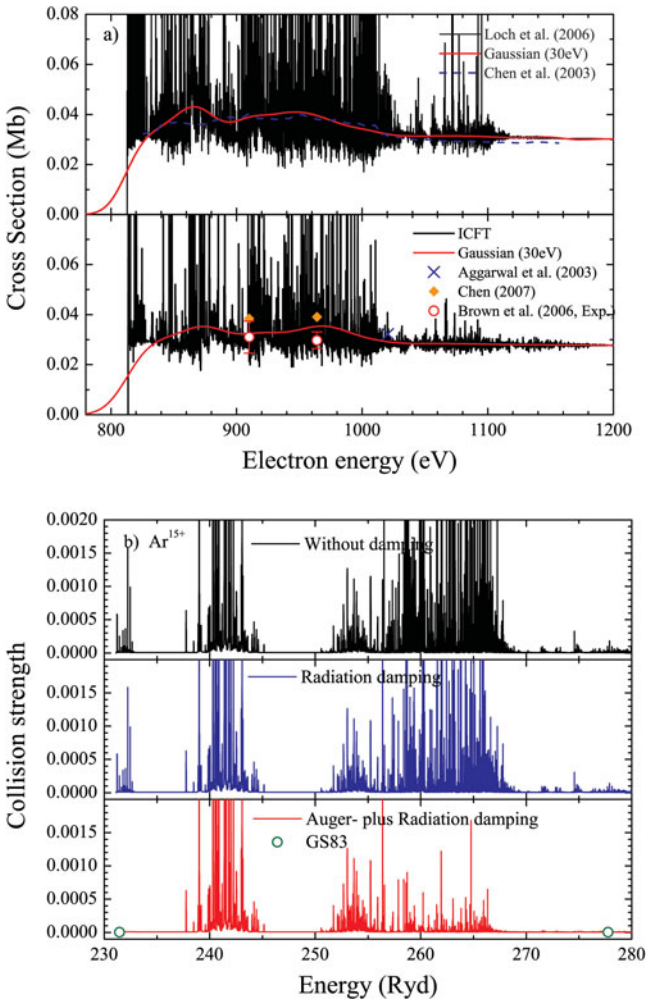

Fig. 5. Comparison of the collision cross sections of (a) Fe^{16+} for $2s^2 2p^6\ ^1S_0 \rightarrow 2s^2 2p^5\ ^3D_1$ ($3D$) excitation between our ICFT R-matrix and previous calculations and (b) Ar^{15+} for $1s^2 2s\ ^2S_{1/2} \rightarrow 1s 2p^2\ ^2P_{1/2}$ excitation.

width of 30 eV, comparable with resolution of present detectors in the laboratory) also shows agreement, except around energies of 870 eV. At energies of 910 and 964 eV, our ICFT *R*-matrix results show a better agreement (6% and 19%) with laboratory measurements[25] than results of Chen[26] (24% and 28%) and Loch et al.[24] (26% and 33%). For Maxwellian averaged collision strength, the Dirac *R*-matrix calculation of Loch et al.[24] is systematically slightly higher than the ICFT *R*-matrix calculation, by ~7%, which is consistent with the difference level of atomic structure, e.g., the *gf*-values of 5.97×10^{-1} and 6.39×10^{-1}, respectively. For Ar^{15+}, a weak nondipole transition line, due to $1s2p^2\ ^2P_{1/2} \rightarrow 1s^2 2s\ ^2S_{1/2}$, was selected to check the accuracy (see Fig. 5b). The background of the ICFT *R*-matrix calculation agrees well with the results of Goett and Sampson.[27] Strong resonances appear as expected for forbidden transitions, which significantly enhances the effective collision strengths. This also demonstrates that Auger and radiation damping effects on Ω are very strong.

A survey comparison with other databases also has been done to investigate the spread of consistency or inconsistency among the different calculations. For core-electron excitations, the Auger-plus-radiation damping effect along the sequence was examined. It is significant and widespread over the entire sequence, and more so for the higher-charge ions. For some inner-shell transitions (39% of available distorted-wave data to $1s^2 2l$ levels in Ar^{15+}), the damped effective collision strengths are still larger than those without the inclusion of resonances (by 20%). The Auger damping effect was found to be dominant in the reduction of resonance enhancement on the electron impact excitation over the entire sequence, whereas the radiation damping is small for lower-charge ions but increases with increasing nuclear charge.

Additionally, we examined the isoelectronic trends of the effective collision strengths by excluding the level crossing effects on the effective collision strength (Y). A complicated pattern of spikes and dips of Y at low temperatures was noted along the sequence for some transitions with strong resonances in these isoelectronic sequences, which precludes the generality of interpolation in Z. With increasing temperature, the resonance effects decrease as expected. Such irregular effects are only popularly seen at low charges and lower-threshold energy transitions.

IV. CONCLUSIONS

We have generated an extensive set of reliable excitation data with the ICFT *R*-matrix method for spectroscopic research in the astrophysical and fusion communities. Moreover, the resultant excitation data along the isoelectronic sequences were assessed to be reliable and could be confidently incorporated into astrophysical and fusion database/modeling codes, such as Chianti, ADAS, AtomDB, etc. The updated modeling code is expected to identify new lines and improve diagnostics, and it may overcome some shortcomings in current astrophysical modeling.

ACKNOWLEDGMENTS

The work of the United Kingdom's APAP network is funded by the U.K. Science and Technology Facilities Council under grant ST/J000892/1 with the University of Strathclyde. G. Y. L. and G. Z. acknowledge the support from the One-Hundred-Talents program of the Chinese Academy of Sciences and the Natural Science Foundation of China under grants 11273032 and 10821061, respectively.

REFERENCES

1. J. H. KASTNER et al., "Evidence for Accretion: High-Resolution X-Ray Spectroscopy of the Classical T Tauri Star TW Hydrae," *Astrophys. J.*, **567**, 434 (2002).

2. B. O'DWYER et al., "SDO/AIA Response to Coronal Hole, Quiet Sun, Active Region, and Flare Plasma," *Astron. Astrophys.*, **521**, A21 (2010).

3. R. O. MILLIGAN, "Spatially Resolved Nonthermal Line Broadening During the Impulsive Phase of a Solar Flare," *Astrophys. J.*, **740**, 70 (2011).

4. M. GÜDEL and Y. NAZÉ, "X-Ray Spectroscopy of Stars," *Astron. Astrophys. Rev.*, **17**, 309 (2009).

5. P. TESTA et al., "Testing EUV/X-Ray Atomic Data for the Solar Dynamics Observatory," *Astrophys. J.*, **745**, 111 (2012).

6. G. DEL ZANNA, "Benchmarking Atomic Data for Astrophysics: Fe XI," *Astron. Astrophys.*, **514**, A41 (2010).

7. G. DEL ZANNA and P. J. STOREY, "Atomic Data for Astrophysics: Fe XIII Soft X-Ray Lines," *Astron. Astrophys.*, **543**, A144 (2012).

8. G. DEL ZANNA, "Benchmarking Atomic Data for Astrophysics: A First Look at The Soft X-Ray Lines," *Astron. Astrophys.*, **546**, A97 (2012).

9. F. PAERELS et al., "High-Resolution Spectroscopy of the X-Ray-Photoionized Wind in Cygnus X-3 with the Chandra High-Energy Transmission Grating Spectrometer," *Astrophys. J.*, **533**, L135 (2000).

10. K. DENNERL et al., "First Observation of Mars with XMM-Newton High Resolution X-Ray Spectroscopy with RGS," *Astron. Astrophys.*, **451**, 709 (2006).

11. A. R. FOSTER et al., "Updated Atomic Data and Calculations for X-Ray Spectroscopy," *Astrophys. J.*, **756**, 128 (2012).

12. D. C. GRIFFIN et al., "*R*-Matrix Electron-Impact Excitation Cross Sections in Intermediate Coupling: An MQDT

Transformation Approach," *J. Phys. B: At. Mol. Opt. Phys.*, **31**, 3713 (1998).

13. N. R. BADNELL and D. C. GRIFFIN, "Electron-Impact Excitation of Fe^{20+}, Including $n = 4$ Levels," *J. Phys. B: At. Mol. Opt. Phys.*, **34**, 681 (2001).

14. M. C. WITTHOEFT et al., "*R*-Matrix Electron-Impact Excitation Calculations Along the F-Like Iso-Electronic Sequence," *J. Phys. B: At. Mol. Opt. Phys.*, **40**, 2969 (2007).

15. N. R. BADNELL, "Dielectronic Recombination of Fe^{22+} and Fe^{21+}," *J. Phys. B: At. Mol. Opt. Phys.*, **19**, 3827 (1986).

16. G. Y. LIANG and N. R. BADNELL, "*R*-Matrix Electron-Impact Excitation Data for the Ne-Like Iso-Electronic Sequence," *Astron. Astrophys.*, **518**, A64 (2010).

17. A. D. WHITEFORD et al., "A Radiation-Damped *R*-Matrix Approach to the Electron-Impact Excitation of Helium-Like Ions for Diagnostic Application to Fusion and Astrophysical Plasmas," *J. Phys. B: At. Mol. Opt. Phys.*, **34**, 3179 (2001).

18. G. Y. LIANG and N. R. BADNELL, "*R*-Matrix Electron-Impact Excitation Data for the Li-Like Iso-Electronic Sequence Including Auger and Radiation Damping," *Astron. Astrophys.*, **528**, A69 (2011).

19. G. Y. LIANG et al., "*R*-Matrix Electron-Impact Excitation Data for the B-Like Iso-Electronic Sequence," *Astron. Astrophys.*, **547**, A87 (2012).

20. G. Y. LIANG et al., "*R*-Matrix Electron-Impact Excitation Data for the Na-Like Iso-Electronic Sequence," *Astron. Astrophys.*, **500**, 1263 (2009).

21. E. LANDI et al., "CHIANTI—An Atomic Database for Emission Lines. XII. Version 7 of the Database," *Astrophys. J.*, **744**, 99 (2012).

22. A. D. WHITEFORD et al., "Excitation of Ar^{15+} and Fe^{23+} for Diagnostic Application to Fusion and Astrophysical Plasmas," *J. Phys. B: At. Mol. Opt. Phys.*, **35**, 3729 (2002).

23. H. L. ZHANG et al., "Relativistic Distorted-Wave Collision Strengths and Oscillator Strengths for the 85 Ions with $8 \leq Z \leq 92$," *At. Data Nucl. Data Tables*, **44**, 31 (1990).

24. S. D. LOCH et al., "The Effects of Radiative Cascades on the X-Ray Diagnostic Lines of Fe^{16+}," *J. Phys. B: At. Mol. Opt. Phys.*, **39**, 85 (2006).

25. G. V. BROWN et al., "Energy-Dependent Excitation Cross Section Measurements of the Diagnostic Lines of Fe XVII," *Phys. Rev. Lett.*, **96**, 253201 (2006).

26. G. X. CHEN, "Converged Dirac *R*-Matrix Calculation of Electron Impact Excitation of Fe XVII," *Phys. Rev. A*, **76**, 062708 (2007).

27. S. J. GOETT and D. H. SAMPSON, "Collision Strengths for Inner-Shell Excitation of Li-Like Ions from Levels of the $1s^2 2s$ and $1s^2 2p$ Configurations to Levels of the $1s2l2l'$ Configurations," *At. Data Nucl. Data Tables*, **29**, 535 (1983).